

## **Supplementary Material**

### **SIZE AND DENSITY MEASUREMENTS OF SINGLE SICKLE RED BLOOD CELLS USING MICROFLUIDIC MAGNETIC LEVITATION**

Utku Goreke,<sup>1</sup> Allison Bode,<sup>1,2</sup> Sena Yaman,<sup>4</sup> Umut A. Gurkan,<sup>1,3\*</sup> Naside Gozde Durmus<sup>4\*</sup>

<sup>1</sup>Department of Mechanical and Aerospace Engineering, Case Western Reserve University, Cleveland, OH, USA

<sup>2</sup>Department of Hematology and Oncology, School of Medicine, Case Western Reserve University, Cleveland, OH, USA

<sup>3</sup>Department of Biomedical Engineering, Case Western Reserve University, Cleveland, OH, USA

<sup>4</sup>Molecular Imaging Program at Stanford (MIPS), Department of Radiology, Stanford University, Stanford, CA, USA

#### **\*Corresponding Authors:**

##### **Umut A. Gurkan, Ph.D.**

Warren E. Rupp Associate Professor  
Mechanical and Aerospace Engineering  
Biomedical Engineering  
Case Western Reserve University  
[umut@case.edu](mailto:umut@case.edu)

##### **Naside Gozde Durmus, Ph.D.**

Assistant Professor  
Department of Radiology  
Molecular Imaging Program at Stanford (MIPS)  
Stanford University School of Medicine  
3165 Porter Drive, Palo Alto, CA 94304  
[gdurmus@stanford.edu](mailto:gdurmus@stanford.edu)

This research was, in part, funded by the National Institutes of Health (NIH) Agreement OT2HL152643. The views and conclusions contained in this document are those of the authors and should not be interpreted as representing the official policies, either expressed or implied, of the NIH.

## Underlying physics for magnetic levitation of red blood cells in MagDense:

During magnetic levitation of cells in a microcapillary, MagDense monitors the levitation pattern and distribution of each individual red blood cell in real-time. It magnetically focuses and separates healthy and sickled red blood cells at different positions along the z-direction, based on their magnetic signatures and densities.

During levitation, magnetic force ( $\mathbf{F}_{mag}$ ), buoyancy force ( $\mathbf{F}_b$ ) and drag forces ( $\mathbf{F}_d$ ) are acting on the individual red blood cells are calculated:

$$F_{mag} + F_b + F_d = 0 \quad (\text{Eq.1})$$

$\mathbf{F}_{mag}$  acting on the cells are calculated as:<sup>1</sup>

$$F_{mag} = (m \cdot \nabla) B \quad (\text{Eq.2})$$

$\mathbf{B}$  is the magnetic induction,  $\nabla$  is the del operator and  $\mathbf{m}$  is the magnetic moment, calculated as:

$$m = \frac{V \Delta \chi}{\mu_0} B \quad (\text{Eq.3})$$

$V$  is the volume of the cell, and  $\mu_0$  is the permeability of the free space ( $1.2566 \times 10^{-6} \text{ kg m A}^{-2} \text{ s}^{-2}$ ).

$\Delta \chi$  is the magnetic susceptibility difference between the cell and paramagnetic medium.

$\mathbf{B}$  induced in the channel by opposing magnets in the levitation setup.

During magnetic levitation, cell gained velocity  $\mathbf{v}$  and  $\mathbf{F}_d$  is exerted on the cell.

$\mathbf{F}_d$  is calculated for spherical object as follows:<sup>1</sup>

$$F_d = 6\pi R \eta f_D v \quad (\text{Eq. 4})$$

$R$  is the radius of the cell.

$\eta$  is the dynamic viscosity of the paramagnetic medium.

$f_D$  is the drag coefficient.  $f_D = 1$ , when the cell is far away from the channel wall.

$\mathbf{F}_b$  is calculated as:<sup>2</sup>

$$F_b = V \Delta \rho g \quad (\text{Eq. 5})$$

$\mathbf{g}$  is the gravitational acceleration ( $9.8 \text{ ms}^{-2}$ ), in z-direction.

$\rho$  is the difference between the volumetric densities of the cell and the paramagnetic medium.

In the MagDense setup, cells are focused on  $x=0$  plane where  $B_x=0$  with magnetic forces. On the other hand, the cell levitates in a certain height in  $z$  direction along  $x=0$  plane until magnetic and buoyancy forces come into balance. Thus, during magnetic levitation, the equilibrium height of a cell along the channel height is calculated based on magnetic induction values  $B$ :<sup>2-4</sup>

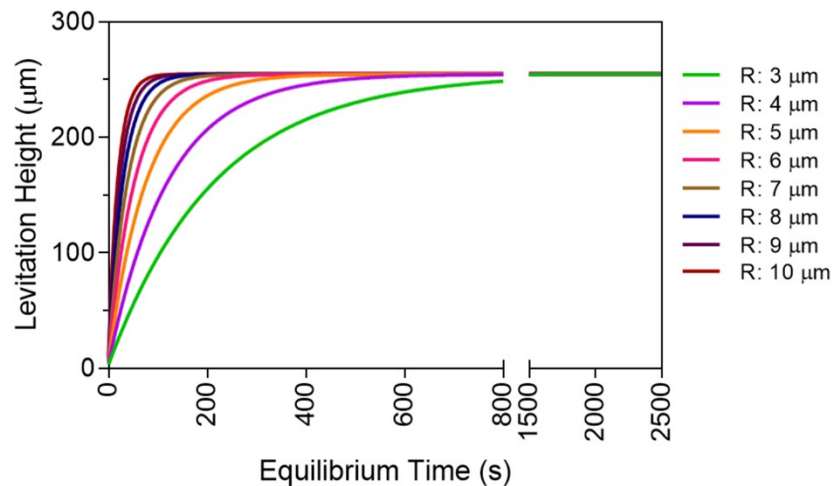
$$F_{mag} + F_b = 0 \quad (\text{Eq. 6})$$

$$\frac{\Delta\chi}{\mu_0} \left( B_x \frac{\partial B_z}{\partial x} + B_y \frac{\partial B_z}{\partial y} + B_z \frac{\partial B_z}{\partial z} \right) - \Delta\rho g = 0 \quad (\text{Eq. 7})$$

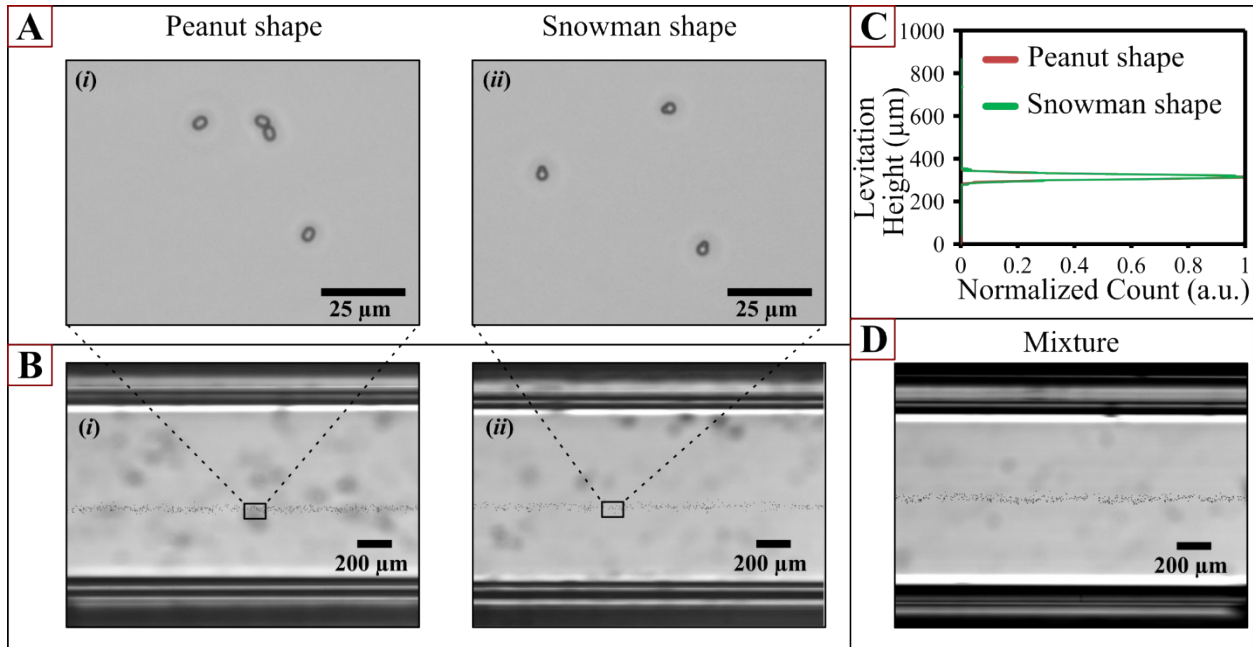
The gravitational acceleration is represented by  $g$ ,  $\mu_0$  defines the permeability of the free space.  $\nabla\rho$  represents the volumetric density difference between the red blood cell and paramagnetic medium (*i.e.*,  $\rho_c - \rho_m$ ) and  $x$ ,  $y$ , and  $z$  are the coordinates of a levitating red blood cell.

#### Effect of cell size on levitation height and equilibration time:

According to Eq. 7, equilibrium levitation height of cells is independent from the cell radius. However, the radius is effective in the drag force,  $F_d$ , which is exerted on cells until they reach their equilibrium position. By constructing a time-dependent model using the magnetic induction data obtained from FEM simulations, the levitation time of healthy red blood cells (1.089 g/mL) with different radii ( $R$ : 3-10  $\mu\text{m}$ ) were calculated with a custom-coded MATLAB file. Dynamic viscosity of the paramagnetic medium,  $\eta$ , and the drag coefficient,  $f_D$ , in  $F_d$  were taken as  $1.105 \times 10^{-3}$  Pa.s and 1, respectively. According to the simulation results, the bigger the size of the cells, the faster they reach their final levitation position. On the other hand, cell size had no effect on the equilibrium levitation height, consistent with Eq. 7.



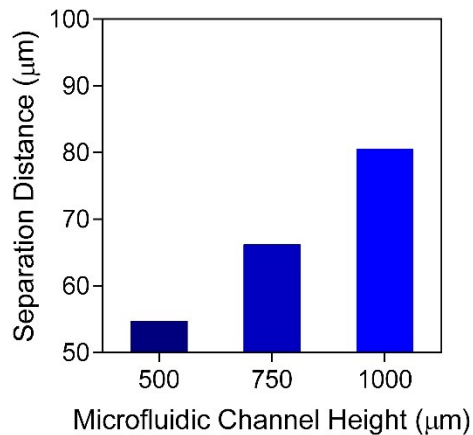
**Supplementary Fig 1. Simulation results for the time required for red blood cells to reach equilibrium.** The cells with same density (*i.e.*, 1.089 g/ml) with different radii (3-10  $\mu\text{m}$ ) reach equilibrium levitation height at 30 mM paramagnetic medium at different times. Equilibrium times are longer for particles cells with smaller radii.



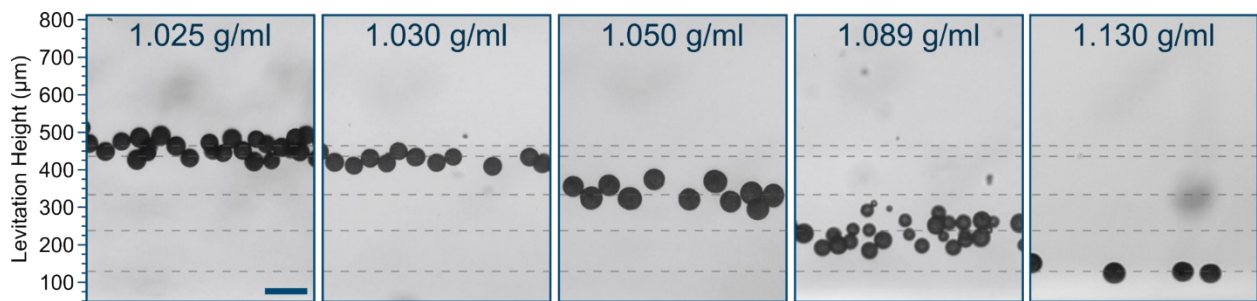
**Supplementary Figure 2. The effect of bead shape on density assay. (A)** 4 μm polystyrene beads with (i) peanut (ii) and snowman shapes. **(B)** Levitation profiles of (i) peanut (ii) and snowman shaped beads. **(C)** Levitation heights peanut and snowman shaped beads coincide. **(D)** Levitation of a mixture of beads with different shapes. The mixture levitated as a single uniform band.

### Theoretical separation distance between healthy and sickle red blood cells in different device dimensions:

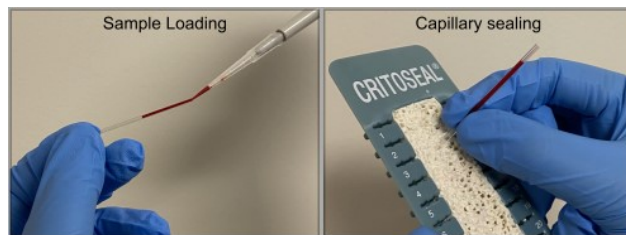
To investigate the effect of device dimensions on the separation distance between HbAA and HbSS cells, magnetic induction inside the microcapillary channel, shown in Eq. 7, was modeled using a finite element modeling tool for different microchannel heights (i.e., 500, 750 and 1000 μm) with a 200-μm channel thickness. In the model, residual magnetic induction ( $B_r$ ) of the N52 grade neodymium magnets was taken as 1.45 T according the manufacturer's data. As lengths of the magnets are long enough compared to their widths, the change of magnetic induction along y axis can be neglected. Contribution of the magnetic susceptibility of the cells in the  $\Delta\chi$  term is negligible compared to that of the paramagnetic medium<sup>5,6</sup>. In the model, the density and molar magnetic susceptibility of the levitation medium were taken as 1.025 g/mL (i.e., serum density) and  $3.2 \times 10^{-4} \text{ M}^{-1}$ , respectively<sup>5</sup>. After constructing the model, levitation heights of healthy (HbAA) and sickle (HbSS) red blood cells, whose densities were determined with the MagDense device, were calculated for 30 mM paramagnetic medium using an in-house developed MATLAB file. The results revealed that separation distance of 1,000 μm, which was tested throughout this work, yields a higher separation distance between the healthy and sickle red blood cells when compared to smaller device configurations.



**Supplementary Figure 3. The effect of channel dimensions on separation of HbAA and HbSS red blood cells.** Bars show theoretical separation distance between healthy red blood cells (1.089 g/mL) and sickle cells (1.110 g/mL) for 500 μm, 750 μm, and 1,000 μm channel heights.



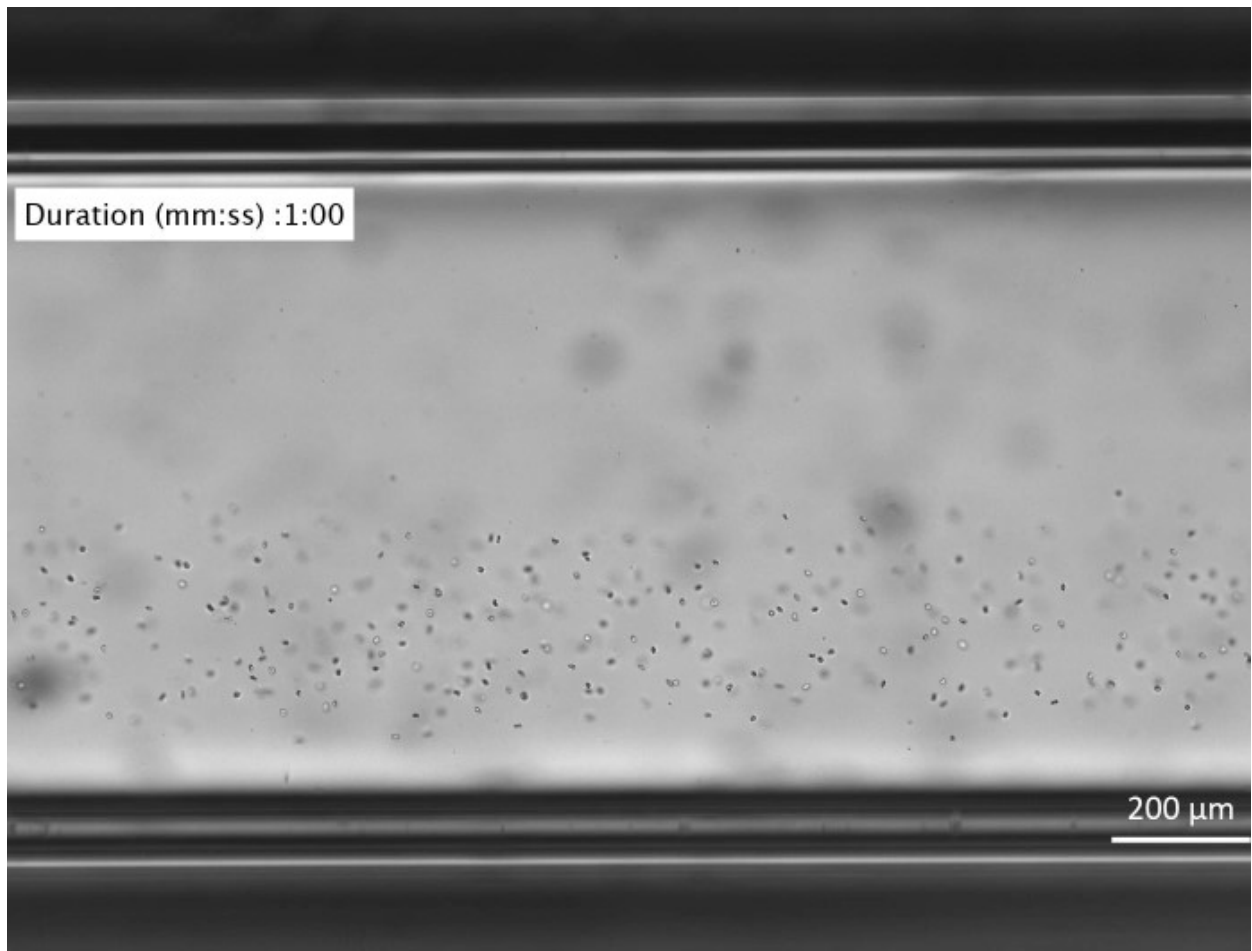
**Supplementary Figure 4. Calibration and assessment of MagDense platform with beads with known densities.** The MagDense device was calibrated with the reference polyethylene beads with known densities (i.e., 1.025 g/mL, 1.030 g/mL, 1.050 g/mL, 1.089 g/mL, 1.13 g/mL). Each reference bead had a distinct levitation height in 30 mM paramagnetic medium, as a function of their density.



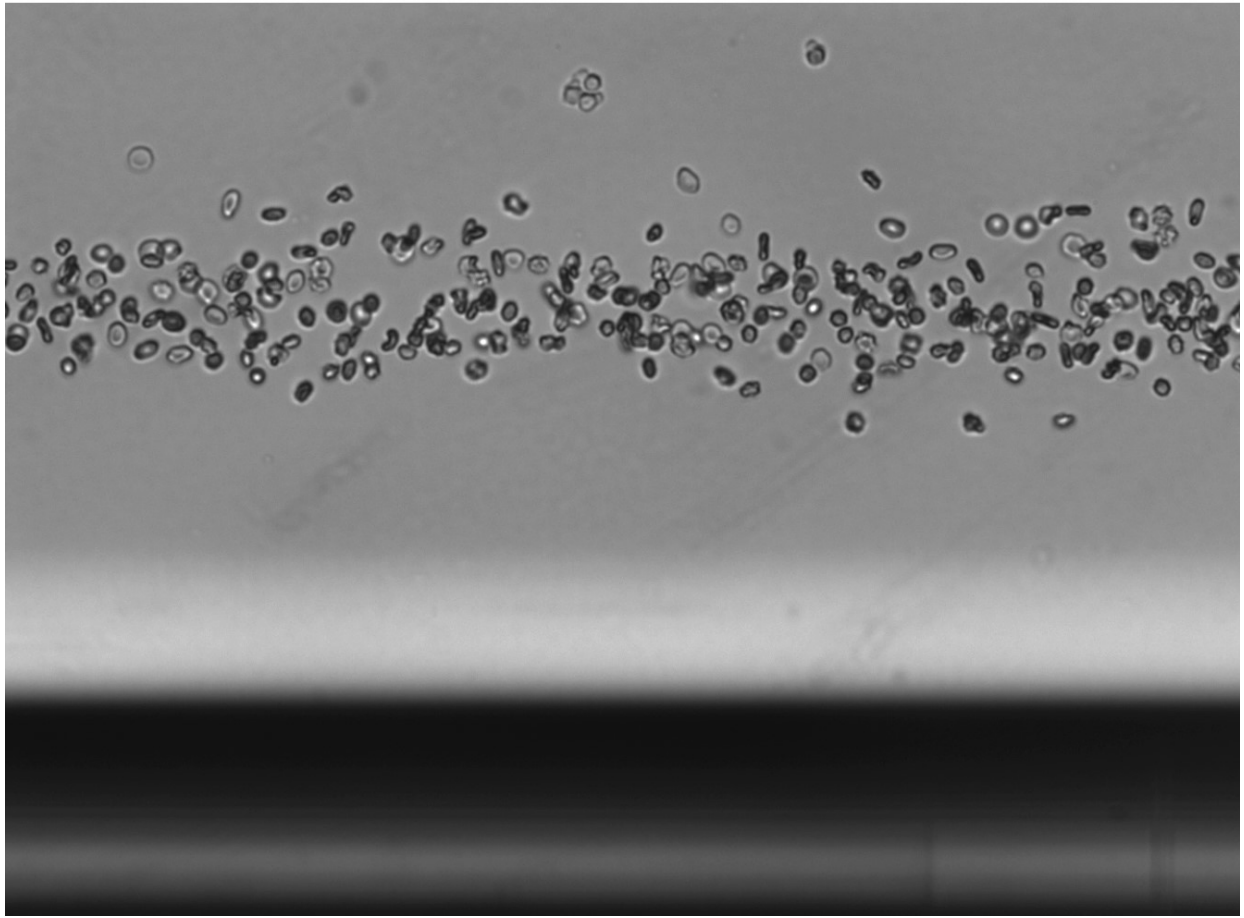
**Supplementary Figure 5. Sample preparation steps.** Samples are loaded into the glass capillary with a pipettor. Both ends of the glass capillary are then sealed with Critoseal®. Glass capillary is then loaded into the MagDense device, as sandwiched between the two magnets.

**Supplementary Table 1. Density fraction details of HbSS SCD subjects.**  $D_{50}$ , shown in increasing order, denotes the median density. Fractions of dense RBCs are shown for different thresholds (1.12 g/ml and 1.11 g/ml). Additionally, fractions of RBCs within 0.01 density brackets are shown with green color scale for each HbSS SCD subject.

| HbSS SCD Subjects | $D_{50}$ | <u>D&gt;1.12</u><br>All | <u>D&gt;1.11</u><br>All | <u>D&lt;1.09</u><br>All | <u>1.10&gt;D&gt;1.09</u><br>All | <u>1.11&gt;D&gt;1.10</u><br>All | <u>1.12&gt;D&gt;1.11</u><br>All | <u>1.13&gt;D&gt;1.12</u><br>All | <u>1.14&gt;D&gt;1.13</u><br>All | <u>D&gt;1.14</u><br>All |
|-------------------|----------|-------------------------|-------------------------|-------------------------|---------------------------------|---------------------------------|---------------------------------|---------------------------------|---------------------------------|-------------------------|
| Subject 1         | 1.0927   | 0.00                    | 0.01                    | 0.35                    | 0.48                            | 0.15                            | 0.01                            | 0.00                            | 0.00                            | 0.00                    |
| Subject 2         | 1.0930   | 0.00                    | 0.01                    | 0.37                    | 0.39                            | 0.23                            | 0.01                            | 0.00                            | 0.00                            | 0.00                    |
| Subject 3         | 1.0981   | 0.01                    | 0.04                    | 0.09                    | 0.51                            | 0.36                            | 0.03                            | 0.01                            | 0.00                            | 0.00                    |
| Subject 4         | 1.1008   | 0.00                    | 0.12                    | 0.06                    | 0.40                            | 0.42                            | 0.12                            | 0.00                            | 0.00                            | 0.00                    |
| Subject 5         | 1.1031   | 0.03                    | 0.26                    | 0.04                    | 0.33                            | 0.37                            | 0.23                            | 0.03                            | 0.00                            | 0.00                    |
| Subject 6         | 1.1075   | 0.03                    | 0.39                    | 0.01                    | 0.15                            | 0.45                            | 0.36                            | 0.03                            | 0.00                            | 0.00                    |
| Subject 7         | 1.1088   | 0.24                    | 0.48                    | 0.00                    | 0.15                            | 0.37                            | 0.24                            | 0.19                            | 0.05                            | 0.00                    |
| Subject 8         | 1.1105   | 0.13                    | 0.53                    | 0.00                    | 0.05                            | 0.42                            | 0.40                            | 0.12                            | 0.01                            | 0.00                    |
| Subject 9         | 1.1118   | 0.00                    | 0.70                    | 0.00                    | 0.00                            | 0.30                            | 0.69                            | 0.00                            | 0.00                            | 0.00                    |
| Subject 10        | 1.1132   | 0.31                    | 0.59                    | 0.00                    | 0.13                            | 0.28                            | 0.28                            | 0.24                            | 0.07                            | 0.00                    |
| Subject 11        | 1.1145   | 0.16                    | 0.80                    | 0.00                    | 0.00                            | 0.20                            | 0.64                            | 0.16                            | 0.01                            | 0.00                    |
| Subject 12        | 1.1179   | 0.42                    | 0.81                    | 0.00                    | 0.00                            | 0.19                            | 0.38                            | 0.30                            | 0.10                            | 0.01                    |
| Subject 13        | 1.1192   | 0.47                    | 0.86                    | 0.00                    | 0.01                            | 0.13                            | 0.38                            | 0.38                            | 0.09                            | 0.00                    |
| Subject 14        | 1.1196   | 0.49                    | 0.74                    | 0.01                    | 0.03                            | 0.22                            | 0.25                            | 0.24                            | 0.23                            | 0.03                    |
| Subject 15        | 1.1233   | 0.82                    | 1.00                    | 0.00                    | 0.00                            | 0.00                            | 0.18                            | 0.80                            | 0.02                            | 0.00                    |
| Subject 16        | 1.1280   | 0.69                    | 0.92                    | 0.00                    | 0.00                            | 0.08                            | 0.23                            | 0.22                            | 0.23                            | 0.23                    |
| <b>Mean</b>       | 1.1101   | 0.239                   | 0.515                   |                         |                                 |                                 |                                 |                                 |                                 |                         |
| <b>SD</b>         | 0.0105   | 0.269                   | 0.341                   |                         |                                 |                                 |                                 |                                 |                                 |                         |

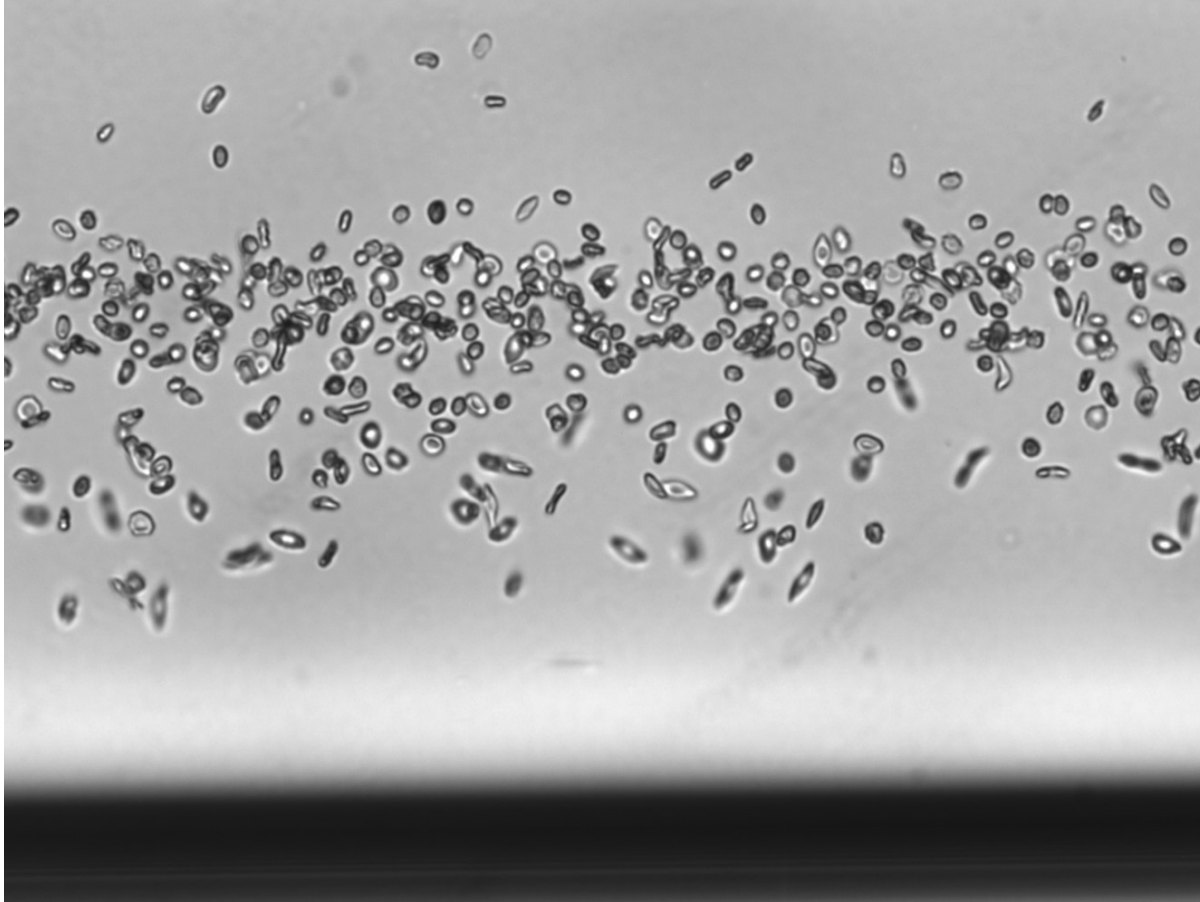


**Supplementary Video 1. Real-time monitoring of levitation of individual red blood cells from a SCD patient in the MagDense platform.** Bright-field microscopy images were taken at every minute for 20 minutes and merged together.



**Supplementary Video 2.** Static levitation and magnetic focusing of red blood cells from a HbAA blood sample at 30 mM paramagnetic medium.





**Supplementary Video 3.** Static levitation and magnetic focusing of red blood cells from a HbSS blood sample at 30 mM paramagnetic medium.

## References

1. H. C. Tekin, M. Cornaglia and M. A. Gijs, *Lab on a Chip*, 2013, **13**, 1053-1059.
2. M. A. Gijs, F. Lacharme and U. Lehmann, *Chemical Reviews*, 2010, **110**, 1518-1563.
3. S. S. Shevkoplyas, A. C. Siegel, R. M. Westervelt, M. G. Prentiss and G. M. Whitesides, *Lab on a Chip*, 2007, **7**, 1294-1302.
4. S. Shim, P. Gascoyne, J. Noshari and K. S. Hale, *Integrative Biology*, 2011, **3**, 850-862.
5. M. J. P. van Osch, E.-j. P. A. Vonken, M. A. Viergever, J. van der Grond and C. J. G. Bakker, *Magnetic Resonance in Medicine*, 2003, **49**, 1067-1076.
6. D. W. Inglis, R. Riehn, J. C. Sturm and R. H. Austin, *Journal of Applied Physics*, 2006, **99**, 08K101.